On the Trade-Off Between Environmental and Economic Objectives in Community Energy Storage Operational Optimization

Wouter L. Schram, Tarek AlSkaif, Ioannis Lampropoulos, Sawsan Henein, and Wilfried G.J.H.M. van Sark

***Abstract*—The need to limit climate change has led to policies that aim for the reduction of greenhouse gas emissions. Often, a trade-off exists between reducing emissions and associated costs. In this article, a multi-objective optimization framework is proposed to determine this trade-off when operating a Community Energy Storage (CES) system in a neighbourhood with high shares of photovoltaic (PV) electricity generation capacity. The Pareto frontier of costs and emissions objectives is established when the CES system would operate on the day-ahead spot market. The emission profile is constructed based on the marginal emissions. Results show that costs and emissions can simultaneously be decreased for a range of solutions compared to reference scenarios with no battery or a battery only focused on increasing self-consumption, for very attractive CO_2 abatement costs and without hampering self-consumption of PV-generated electricity. Results are robust for battery degradation, whereas battery efficiency is found to be an important determining factor for simultaneously decreasing costs and emissions. The operational schedules are tested against violating transformer, line and voltage limits through a load flow analysis. The proposed framework can be extended to employ a wide range of objectives and/or location-specific circumstances.**

***Index Terms*—Community Energy Storage (CES), multi-objective optimization of costs and emissions, marginal emission profiles, PV self-consumption, load flow analysis.**

NOMENCLATURE

Abbreviations

CES	Community Energy Storage
EMS	Energy Management System
PV	Photovoltaics

Indices and Sets

$i \in \mathcal{H}$	Index of Household
$k \in \mathcal{K}$	Bin index of epsilon constraint
n	Half cycle index
$t \in \mathcal{T}$	Time step

Parameters

φ	Battery's coefficient
L_{ca}, L_{cy}	Calendric and cyclic lifetime
M	Big-M constraint
$P_{\mathrm{batt,max}}$	Maximum allowable power to / from battery
$P_{\mathrm{grid,max}}$	Maximum allowable power to / from grid
Q_{cap}	Battery charge capacity
SOC_{max}	Maximum allowable state of charge battery
SOC_{min}	Minimum allowable state of charge battery
r	Cyclic degradation exponent

Variables

ϵ	Epsilon constraint
C_{total}	Total costs
c	Day-ahead market electricity price
DOC	Depth of cycle
D	Degradation
g	CO_2 Emission
m	Battery age
P_{charge}	Charging power
$P_{discharge}$	Discharging power
P_{grid}	Power to / from grid
$P_{L,agg}$	Aggregated residual load
$P_{S,agg}$	Aggregated surplus PV power
SOC	State of charge battery
x	Net PV power surplus (binary)
y	Fraction of PV surplus that fits in battery

Manuscript received July 12, 2019; revised October 17, 2019 and January 13, 2020; accepted January 17, 2020. Date of publication January 27, 2020; date of current version September 18, 2020. This work was part of the Co-Evolution of Smart Energy Products and Services (CESEPS) project, and PARticipatory platform for sustainable ENergy managemenT (PARENT), which received funding in the framework of the joint programming initiative ERA-Net Smart Grids Plus, and the PVProsumers4Grid Project, which received funding from the European Union's Horizon 2020 research and innovation programme under Grant 764786. Paper no. TSTE-00767-2019. *(Corresponding author: Wouter Schram.)*

W. L. Schram, T. AlSkaif, I. Lampropoulos, and W. G.J.H.M. van Sark are with the Copernicus Institute Copernicus Institute of Sustainable Development, Utrecht University, 3584 CS Utrecht, The Netherlands (e-mail: w.l.schram@uu.nl; t.a.alskaif@uu.nl; i.lampropoulos@uu.nl; W.G.J.H.M.vansark@uu.nl).

S. Henein is with the Austrian Institute of Technology, 1210 Vienna, Austria (e-mail: Sawsan.Henein@ait.ac.at).

Color versions of one or more of the figures in this article are available online at https://ieeexplore.ieee.org.

Digital Object Identifier 10.1109/TSTE.2020.2969292

I. INTRODUCTION

IN RECENT years, there has been a sharp increase in the deployment of Photovoltaic (PV) systems for generating electricity. While this plays an important role to mitigate climate change, it can also pose challenges, such as voltage fluctuations and grid capacity issues, when large amounts of PV-generated electricity are simultaneously fed into the grid. Therefore, emphasis has recently been placed on the self-consumption of PV-generated electricity in households [1], [2]. To encourage

self-consumption the surplus injected PV electricity is not remunerated in some countries, and thus potential revenue for prosumers is lost [2]. An option to maximize PV self-consumption is to deploy batteries in households by storing surplus of PV-generated electricity during the day to use it in the evening.

Instead of installing a battery in every household, deploying a Community Energy Storage (CES) system is emerging as an alternative and more cost-effective solution in residential communities because of scale advantages and lower installation costs [3], [4]. For example, when providing ancillary services, a CES system would require only one measurement and communication system and battery Energy Management System (EMS) whereas aggregating individual batteries would require these with every battery. CES systems can result in higher utilization of renewable energy sources [1], [4]–[6], and provide ancillary services to grid operators; such as balancing, peak shaving, load levelling, large-scale integration of renewable energy sources, voltage optimization, and reliability improvement [7]–[9]. Furthermore, CES can play an integral role in DC micro-grids [10].

Several lines of evidence suggest that coupling a PV system with energy storage can be economically attractive, with the most important economic parameters that determine the economic viability being the battery investment costs and the self-consumption benefits (i.e., the difference between the retail electricity price and the PV electricity feed-in tariff). Viable business cases for battery systems have been found by combining a battery price of 781 €/kWh investment costs and 0.26 €/kWh self-consumption benefits [11], investment costs between 265 and 465 €/kWh combined with self-consumption benefits of 0.25 €/kWh to 0.34 €/kWh [12], and investment costs of 234 €/kWh combined with self-consumption benefits of 0.16 €/kWh [13]. However, it is uncertain whether such economic circumstances will arise in the future. Therefore, scholars have shifted their attention on multi-revenue applications of energy storage [14], for example the hierarchical optimization for energy arbitrage in the day-ahead spot market and the contribution in system balancing [15], and the combination of self-consumption benefits and provision of frequency restoration reserves [16]. In this research, the use of a CES for PV self-consumption is expanded by two other applications, namely minimizing electricity costs on the day-ahead market and minimizing the emissions associated with the consumption of electricity.

Many studies see a role for batteries in mitigating climate change in an indirect manner, namely by supporting the integration of renewable energy [17], [18]. Fares and Webber [19] found that integrating a PV system with a battery can actually increase CO_2 emissions, mainly because of the conversion losses that result in a higher electricity demand. This stresses the importance of addressing the impact on CO_2 emissions that are related to the operation of a battery system. Given that the operator of a sufficiently large CES can purchase/sell electricity from/to the grid, e.g., based on forecasted day-ahead spot market prices, this can be done by converting emissions to costs and incorporating these in a cost minimization approach [20]. An alternative is to incorporate time-varying CO_2 emission factors as input data, which enables the separate minimization of emissions. In this regard, the Pareto frontier can be used to address the trade-off between different objectives [21], for example to decide between different energy devices for satisfying heat and electricity demand [22]. The Pareto frontier has been applied to address the trade-off between costs and emissions in portfolio optimization [23] and for demand side management of flexible load [24]. In this research, we establish a multi-objective optimization framework based on the Pareto frontier approach to demonstrate the trade-off between economic and environmental objectives for the operation of a CES system, using a spot market electricity price profile and a marginal emission profile as inputs.

This paper anticipates on a future energy system with a high share of decentralized energy sources, and the possibility for residential prosumers to collectively own a battery system. This entails new market designs such as decentralized electricity markets (also called local markets), energy communities and microgrids. In these designs, regulation and other economic arguments – such as licensing and certification, data and employment regulation – are fundamental but still open topics. In the current regulatory environment, multiple CES systems should be coupled through an aggregator to meet the entrance requirements of a specific electricity market.

The contribution of our research is threefold. Firstly, to our knowledge, it is the first study to use marginal emission profiles as input for optimization, instead of hourly average profiles. As we elaborate on later, the use of marginal emission profiles reflects reality more accurately for the specified application. Secondly, we demonstrate the impact of important battery characteristics like battery degradation and efficiency on the Pareto frontier of optimal solutions for a multi-objective optimization of costs and emissions. In addition, since we treat self-consumption of PV-generated electricity as a constraint, this becomes effectively the third purpose of the battery (next to cost and emission optimization), which is a novel approach. Thirdly, we assess whether the use of our algorithms lead to violation of grid constraints based on a load-flow analysis.

The paper is structured as follows: The methods are presented in Section II. The numerical evaluation of the proposed framework is presented in Section III. We conclude the paper and provide recommendations for future research directions and some limitations in Section IV.

II. Methods

A. System Layout and Boundaries

The topology and system boundaries of the investigated community are shown in Fig. 1. We modelled interaction between the a CES and H households, indexed by i, where $i \in \mathcal{H} = \{1, 2, \ldots, H\}$, each with an on-site PV system (i.e., prosumers). Households are connected to the main grid and to a CES in their neighbourhood via AC power lines. The surplus PV-generated electricity is stored in the CES that is controlled by an EMS. The EMS is responsible for optimizing the day-ahead charging schedule, in order to satisfy the households' residual load, while accommodating their aggregated surplus PV-generated electricity. Households are connected to the main grid to secure their residual load during times when PV-generated electricity is not sufficient and there is no available energy stored in the CES.

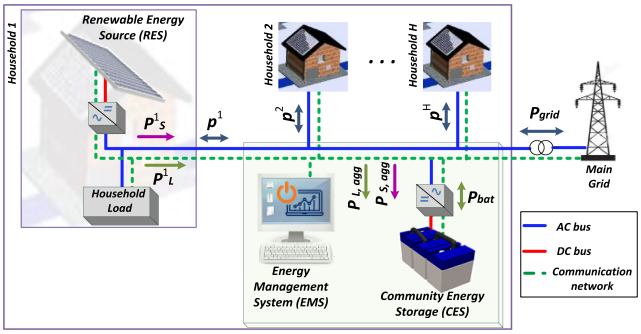

Fig. 1. Scheme of the considered system layout.

In a certain time slot, the community could either store some of its surplus PV-generated electricity in the CES, or request energy from the battery for satisfying its residual load. The average power of household i for time step $t \in \mathcal{T} = \{t_0, t_0 + \Delta t, t_0 + 2\Delta t, \ldots, T\}$ is denoted as $P^{t,i}$. In the remainder, all power flows P are in [kW]. The duration between two consecutive time steps is Δt, which can represent different timescales (e.g., one hour). The community power P^t_{agg} is an aggregation of the net loads of all households at time step t:

$$P^t_{\text{agg}} = \sum_{i=1}^{H} P^{t,i}. \tag{1}$$

P^t_{agg} represents either a net surplus PV power $P^t_{\text{S,agg}}$ (i.e., $P^t_{\text{agg}} < 0$) or a net amount of power demand for residual load $P^t_{\text{L,agg}}$ (i.e., $P^t_{\text{agg}} > 0$). Hence, we define residual load as a non-negative value where PV-generated power is subtracted from the actual load, whereas we define surplus PV power as a non-negative value where actual load is subtracted from PV-generated power.

B. Battery Degradation

Battery performance is affected over time and upon usage [25]. Important battery parameters that decline are the efficiency (e.g., through the increase of internal resistance), the pulse power capability and the capacity [26]. Regarding capacity fading, two important battery ageing components are cyclic ageing and calendric ageing. These processes occur independently from each other and thus should be added together to obtain the total degradation [11], [26]. According to [11], calendric ageing is linearly dependent on time. The relation between ageing and charging cycles is less straightforward. Wöhler curves (also called S-N curves, reflecting Stress and Number of cycles) are historically used to predict the material fracture under cycle loading [27]. Using these has also become common practice in estimating the number of full-equivalent cycles (FECs) a battery can withhold as a function of depth of cycle (*DOC*) [11], [28], [29]. The basic notion is that with equal energy throughput, smaller DOCs lead to reduced aging compared to larger DOCs. From [11], we can derive (2) to estimate the cumulative degradation D^m (in %) at the m^{th} day of battery operation:

$$D^m = 20\% * \left(\frac{m}{L_{\text{ca}}} + \sum_{n=1}^{N} \frac{0.5}{L_{\text{cy}} * DOC_n^{r-1}} \right) \tag{2}$$

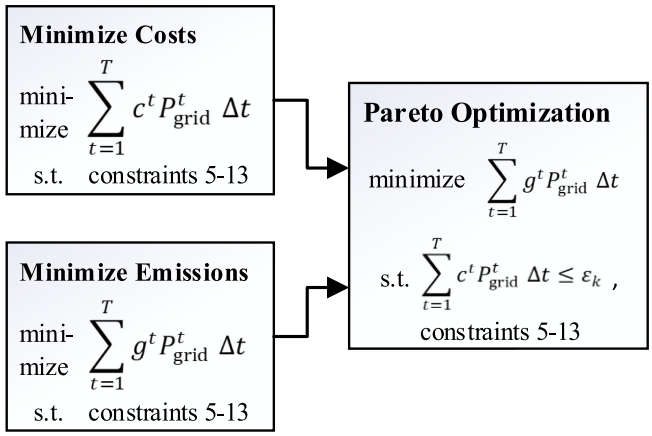

Fig. 2. Schematic representation optimization process

Herein, 20% reflects the capacity loss that is generally considered end of life. The quotient of battery age m (in [days]) and calendric lifetime L_{ca} (in [days]) denotes the calendric ageing. Cyclic ageing is estimated by summing the incremental degradation of each half[1] cycle $n \in \{1, 2, \ldots, N\}$ in which N is the number of half cycles since the start of battery operation. L_{cy} is the number of FECs if *DOC* would be 100% for every cycle and r is the cyclic degradation exponent that corrects for actual cycle depth. Using (2) and assumptions on the parameters' values (see Section III.A), we update the remaining battery capacity in our model every day.

C. Optimization Problem Formulation

1) Pareto Frontier and ϵ-Constraint Method: The main objective is to find a trade-off between electricity cost and CO_2 emissions when setting a charging schedule for the CES. This trade-off can be studied through the Pareto frontier. In the proposed scheduling framework, the ϵ-constraint method is used to calculate the Pareto frontier [21]. In this method, first each optimization problem is solved separately (i.e., electricity cost minimization problem and CO_2 emission minimization problem). By doing so, the two endpoints of the Pareto frontier are calculated, and the range of possible electricity cost and CO_2 emissions becomes known. After that, the range of electricity cost is divided into K equally spaced bins ϵ_k, where $k \in \mathcal{K}\{1, 2, \ldots, K\}$. The optimization process and minimization functions are visually depicted in Fig. 2.

The electricity cost and CO_2 emission functions can be defined as:

$$C_{\text{total}} = \sum_{t=1}^{T} c^t P^t_{\text{grid}} \Delta t, \tag{3}$$

$$G_{\text{total}} = \sum_{t=1}^{T} g^t P^t_{\text{grid}} \Delta t \tag{4}$$

where P^t_{grid} is the power absorbed from or injected into the grid and c^t is the DAM-price (in [€/kWh]), both at time-slot

[1] Hence the 0.5 in the numerator

t (in [h]). The CO_2 emission function can be described in the same way as the cost function, with c^t replaced by the emission input g^t (in [kg CO_2/kWh]), obtaining total emissions G_{total}. Both the electricity tariff and the CO_2 emissions are considered as demand response signals and are piecewise constant with possible jumps at a subsequent time step.

The objective functions are subject to a number of constraints.

2) Power Conservation: The conservation of power property for the entire system is given by the familiar local balancing formula:

$$P^t_{\text{grid}} + P^t_{\text{S,agg}} + P^t_{\text{discharge}} = P^t_{\text{L,agg}} + P^t_{\text{charge}}, \quad \forall t, \tag{5}$$

where $P^t_{\text{discharge}}$ and P^t_{charge} are the discharging and charging power of the battery.

3) Battery Dynamics: The battery's coefficient φ (in [kWh^{-1}]) is related to the battery charge capacity (i.e., Q_{cap} in [kAh]) and open circuit voltage (i.e., V_{oc} in [V]) as:

$$\varphi = \frac{1}{Q_{\text{cap}} V_{\text{oc}}}. \tag{6}$$

The battery State of Charge *SOC* at time step $t+1$ is a function of P^t_{charge}, $P^t_{\text{discharge}}$ and the *SOC* at time step t, and can be calculated by:

$$SOC^{t+1} = SOC^t + \Delta t \left(\varphi \eta_{\text{c}} P^t_{\text{charge}} - \varphi \frac{P^t_{\text{discharge}}}{\eta_{\text{d}}} \right), \quad \forall t \tag{7}$$

where η_{c} and η_{d} represent the charge and discharge efficiency of the battery, respectively. Equation (7) represents the discrete-time battery dynamics.

The *SOC* of the battery is constrained as follows:

$$SOC_{\min} \leq SOC^t \leq SOC_{\max}, \ \forall t, \tag{8}$$

where $SOC_{\min}$ and $SOC_{\max}$ are the minimum and maximum allowed *SOC* of the battery, respectively. We set these at 0% and 100%, respectively, because we only treat usable capacity.

Besides, a global balance of the battery is included to ensure equal or better conditions for the next day of simulation when the model is run over an extended period of time:

$$SOC^{t=T} \geq SOC^{t_0}. \tag{9}$$

By convention, we set the SOC^{t_0} at 50%.

4) Self-Consumption: A Big-M constraint [30] is used to ensure that the proposed operation of the CES is not at the expense of the self-consumption of PV-generated electricity:

$$y^t P^t_{\text{S,agg}} - P^t_{\text{charge}} \leq M \left(1 - x^t\right), \ \forall t, \tag{10}$$

where x^t is a binary input variable that is 1 when there is surplus PV electricity. On days where the total $P^t_{\text{S,agg}}$ exceeds the battery capacity, this constraint cannot be met without the fraction y^t. This is an input variable that represents the fraction of $P^t_{\text{S,agg}} \Delta t$ that fits in the battery without violating the battery's energy constraints on such days. The value of *M* should be sufficiently large, resulting in that the artificial variable would not be part of any feasible solution.

5) Power Boundaries: Finally, we assume the grid power P^t_{grid} and battery power P^t_{batt} are limited in every time step t according to the following inequality constraints:

$$-P_{\text{grid,max}} \leq P^t_{\text{grid}} \leq P_{\text{grid,max}}, \quad \forall t, \tag{11}$$

$$0 \leq P^t_{\text{charge}} \leq P_{\text{batt,max}}, \quad \forall t, \tag{12}$$

$$0 \leq P^t_{\text{discharge}} \leq P_{\text{batt,max}}, \quad \forall t, \tag{13}$$

where $P_{\text{grid,max}}$ and $P_{\text{batt,max}}$ are the maximal power that can be received from the grid and the battery, respectively.

6) Optimization problem: The ϵ-constraint multi-objective optimization problem [21] can now be formulated as:

$$\begin{aligned} &\text{minimize} \ \sum_{t=1}^{T} g^t P^t_{\text{grid}} \Delta t \\ &\text{s.t.} \quad \sum_{t=1}^{T} c^t P^t_{\text{grid}} \Delta t \leq \epsilon_k, \\ &\qquad \text{constraints (5)–(13).} \end{aligned}$$

D. Battery Targeting Solely PV Self-consumption

The optimal solutions are compared with a reference scenario. The reference scenario in this study is a CES that is solely aimed at increasing the consumption of on-site generated PV electricity; we will denote this as the "Self-consumption only battery". This battery is charged when $P^t_{\text{agg}} < 0$ and discharged when $P^t_{\text{agg}} > 0$. Operation of the battery is controlled using constraints enforced by the battery management system, for example the power and energy constraints of the battery, but no further optimization is applied.

E. Load Flow Analysis

A load flow analysis is performed to assess whether LV grid limits would be violated, for three different optimal schedules. The network used is a Kerber network [31] for suburban areas, using 58 nodes (57 households and one CES) and a 160 kVA transformer station, which is in line with Dutch standards [32]. A time-resolution of five minutes was chosen.

III. Numerical Evaluation

A. Data Input

1) Consumption and Surplus PV Profiles: The consumption and surplus PV profiles are taken from 60 prosumers located in the neighbourhood Nieuwland of the Dutch city of Amersfoort. Net-metered power measurements were obtained as part of the "Smart Grids: Benefit for all" project [33], from 1 November 2013 to 1 October 2014. Data was collected with a time resolution of 10 seconds, but for this research it was averaged over an hour corresponding to the day-ahead market time resolution. Some days were missing, resulting in a representative total of 295 days for the simulation. These data were used to determine how much electricity could be purchased / sold on the wholesale market, and in that sense we implicitly assume perfect information forecasting. The average PV system size is 2.4 kWp

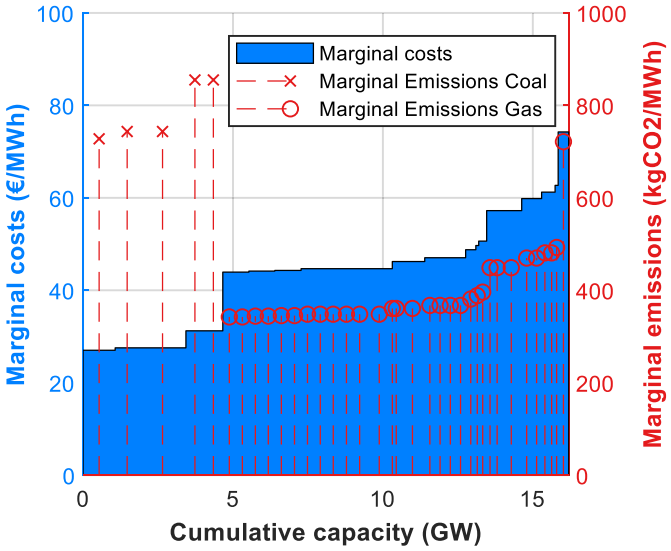

Fig. 3. Marginal costs and emissions of Dutch electricity generation mix in 2014. Source: [36].

(SD = 0.79), with a range from 0.5 kWp to 6.2 kWp. Average annual residual electricity load is 2.5 MWh (SD = 1.1). The maximum PV surplus was 83.7 kWh/h, which was used as $P_{grid,max}$ in the optimization model. This is a conservative constraint, which forces the battery not to discharge excessively in times of high PV electricity generation, and not to charge excessively in times of high electricity demand.

2) Price Profile: Day-ahead market (DAM) prices in the Dutch market of the same period as the obtained load profiles are used [34]. We assume that the community is legally allowed to trade electricity on the wholesale market. As mentioned before, currently this is not possible due to minimum bid size requirements. However, the CES can be operated by an aggregator which owns multiple CESs in different communities and aggregate them all together in order to achieve the minimum bid size requirements.

3) Emission Profile: We use marginal emission factors to construct the marginal emission profile. The concept of marginal emission factors focuses on the notion that renewably generated electricity replaces the electricity generated by the price setting power plants of that same time slot [20], which is generally seen as a superior method over average emission factors [35]. Using average emission factors implicitly assumes that a change in demand results in a small change in generation of all facilities in the generation mix. However, operating flexible demand does not result in changes of the complete generation mix, but merely of the power plant operating at the margin. Hence, the marginal emissions of the system should be used instead of the average emissions. We take the merit order as presented in [36], which provides both the marginal costs and the marginal emissions of each electricity generation facility in the Netherlands (see Fig. 3). Using these data, and following the logic that the marginal operating plant is the plant with marginal costs closest to the market price, the emission profile can be generated as the market price profile is known (see Section III.A.2)) Here, for every time step t a value for the marginal system emission g^t is calculated.

TABLE I
BATTERY SYSTEM CHARACTERISTICS

Parameter	Quantity	Unit	Source
Battery size	205	[kWh]	[12], [13], [43]
$\eta_c = \eta_d$	$\sqrt{0.89}$	-	[39]
C-rate	0.4	[h^{-1}]	[44]
Cycle life L_{cy}	4586	[-]	[11], [39]
Cyclic degradation exponent r	-0.5093	[-]	[11]
Calendric life time L_{ca}	20	years	[45]

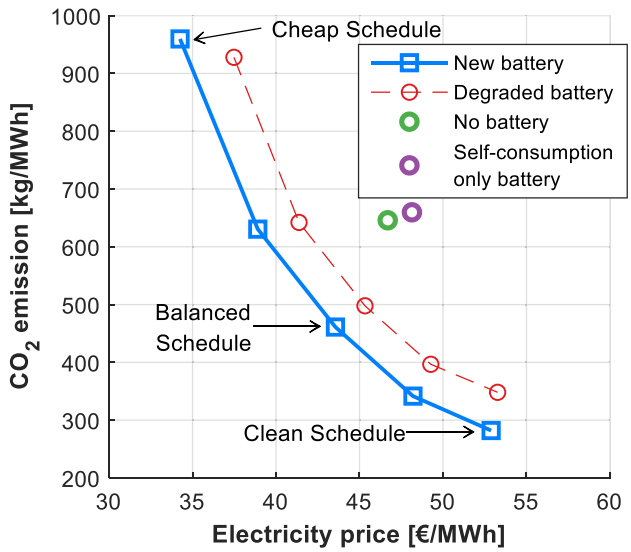

Fig. 4. Pareto front of multi-objective optimization of average DAM price and CO_2 emissions of the community. Reference scenario of the situation without a battery and a self-consumption only battery are also shown, as well as the pareto front of a degraded battery.

4) Battery System Parameters: The technical parameters of the Lithium iron phosphate (LFP) battery CES battery that we use can be found in Table I.

B. Costs and Emissions of Various Operation Schedules

Fig. 4 shows the key results of this work, namely the average electricity costs and accompanying CO_2 emissions in relation to various battery operation schedules for a new battery and a degraded battery. For the new battery, the cheapest operation schedule leads to a cost reduction from 48.1 €/MWh of net electricity consumption of the "Self-consumption only battery", to 34.3 €/MWh; a reduction of 28.8%. However, in this operation the CO_2 emissions would increase from 613 kg/MWh to 960 kg/MWh. The cleanest operation would lead to average emissions of 282 kg/MWh; a reduction of 57.2%. Opting for this operation would lead to an increase in electricity costs to 52.9 €/MWh. There are also many schedules possible that both decrease costs and emissions. For example, in the "Balanced operation", which we define as the operation of the median of ϵ_k, the costs are 43.6 €/MWh (a reduction of 9.5%) and the emissions 464 kg/MWh (a reduction of 29.7%). Hence, this

TABLE II
OPTIMIZATION SCHEDULES VERSUS SELF-CONSUMPTION ONLY BATTERY

Optimization	CO_2 impact (t)	Electricity Costs impact (k€)	CO_2 PBT (years)	CO_2 Abatement costs (€/tCO_2)
Cheapest	+25.5	-1.18	-	-
2nd Cheapest	-2.15	-0.78	>20	-365
Balanced	-16.6	-0.39	2.2	-23.5
2nd Cleanest	-26.8	+0.00	1.3	0.179
Cleanest	-32.1	+0.40	1.1	12.6

operation leads to negative CO_2 abatement costs and can be considered as a no regret option if a CES system is already installed. Table II elaborates on this, presenting cost and emission impact, CO_2 pay-back time (PBT) and CO_2 abatement costs for different Pareto points. The CO_2 PBT entails the period needed to mitigate the emissions associated with production of the battery, which are set at 157 kg CO_2 per kWh battery capacity based on [37]. The 2nd cheapest schedule gives the lowest CO_2 abatement costs, however the CO_2 PBT is high and it is questionable whether that would be within the economic lifetime of the battery. Negative abatement costs are possible because generation is shifted from less efficient to more efficient generating facilities of the same fuel. In this case the cost and emission objective are in synergy as this shift leads to reduction in both costs and emissions. In general, it is apparent that starting from the cheapest operation, large steps in emission reduction can be taken at relatively low costs. The last steps to the cleanest operations entail relatively high costs; this concerns the shift from coal to gas.

A further striking notion from Fig. 4 is that a self-consumption only CES leads to slightly higher electricity costs and emissions than having no CES. This is simply due to efficiency losses that occur when the electricity is converted to chemical energy and vice versa.

After one year of operation, battery degradation is 3.0%, 2.6% and 2.7%, respectively, for the cheapest, balanced and cleanest schedule. Of this, 2.0%, 1.6% and 1.7% can be attributed to the use of the battery (cyclic degradation). The graph of the degraded battery in Fig. 4 depicts the Pareto frontier after five years of operation for the same cost and emission input. Energy and power performance of the battery are decreased with 12.9% to 14.8%. The roundtrip efficiency is assumed to be decreased from 89% to 87.6%, based on [38]. From Fig. 4 it can be concluded that savings on costs and emissions can also be obtained with a degraded battery.

To provide more insight in the battery operation and grid interaction within the three charging schedules that are indicated on the Pareto frontier of Fig. 4 we demonstrate these on a randomly chosen day (1 October 2014) in Fig. 5.

The DAM price and marginal emissions are shown on Fig. 5(a). Fig. 5(b) demonstrates the battery operation and interaction with the grid when the CES control is optimized on cost. The battery is charged from the grid when costs are lowest, for example between 02:00 and 04:00, between 11:00 and 16:00 and between 22:00 and 24:00. When prices are highest (e.g., between

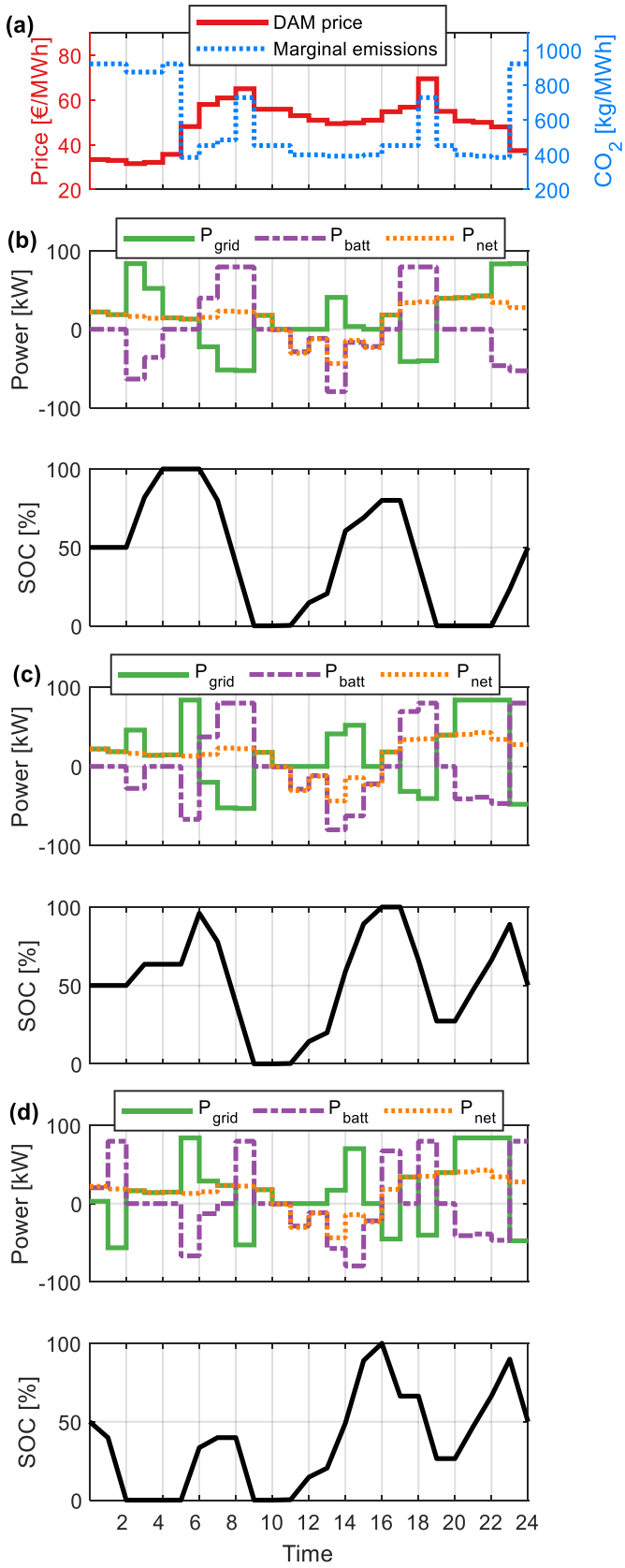

Fig. 5. DAM price of 1 October 2014 and corresponding marginal emissions (a), Cleanest operation and accompanying battery *SOC* (b), Balanced operation and *SOC* (c) and Cheapest operation and *SOC* (d).

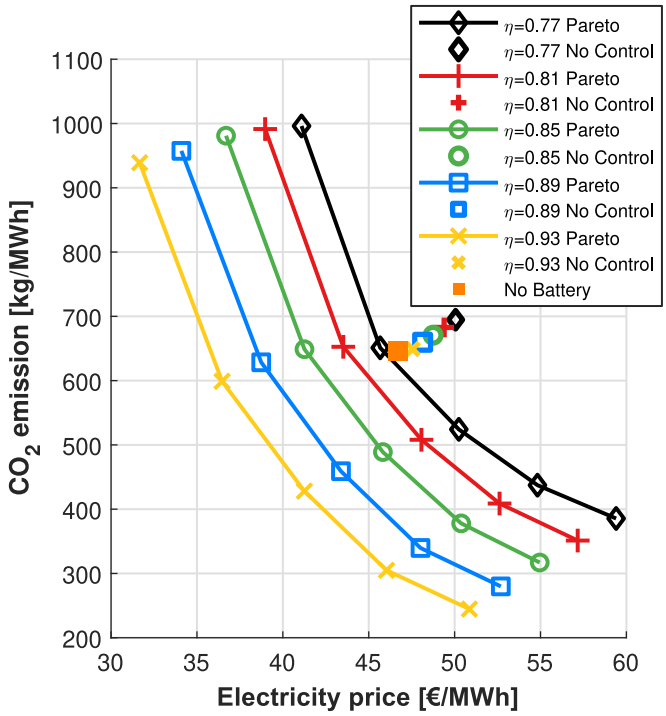

Fig. 6. Impact of round-trip efficiency on pareto frontier.

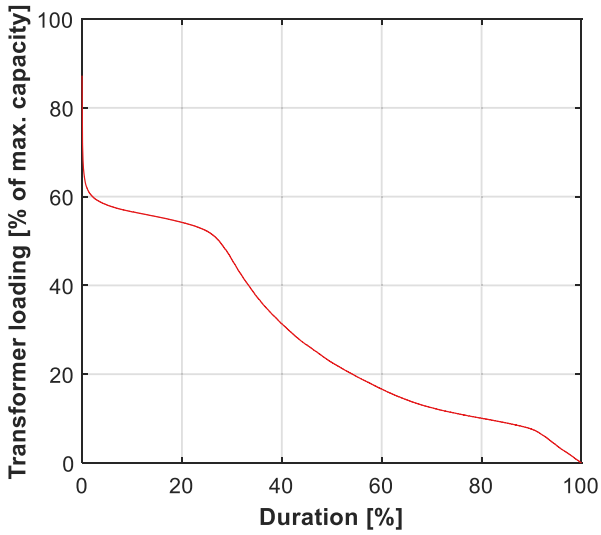

Fig. 7. Transformer loading during load flow simulation at 5-minute time resolution for the balanced schedule.

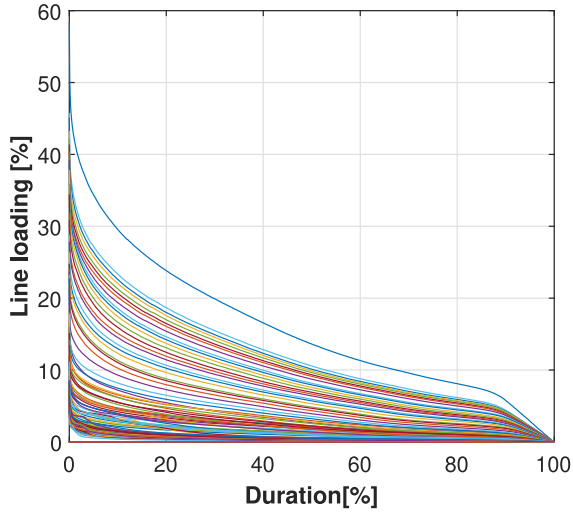

Fig. 8. Line loading at all nodes at 5-minutes time resolution for the balanced schedule.

06:00 and 09:00 and between 17:00 and 19:00, electricity is exported to the grid. Fig. 5(d) shows the community's battery operation and grid interaction when optimized on CO_2 emissions. In contrast to the cheapest schedule, the battery is discharged when marginal emissions are relatively high, for example from 0:00–2:00 and from 23:00–24:00, when a coal-fired power plant is the marginal operating facility, and also from 8:00–9:00 and 16:00–19:00 when an inefficient gas-fired power plant is at the margin. Charging occurs when the marginal emissions are low (between 5:00 and 6:00 and between 21:00 and 23:00), and with self-generated PV electricity (between 11:00 and 16:00) when P_{net} is below zero.

Fig. 5(c) shows the grid interaction and battery operation in the 'balanced schedule'. In contrast to the cheapest and cleanest operation, note that the battery is barely used between 0:00 and 5:00. The battery is charged whenever an efficient gas-fired power plant is marginal, i.e., between 5:00 and 6:00, in the afternoon and between 20:00 and 23:00.

Fig. 5(b)–(d) all show that the battery operation does not hamper the self-consumption of PV electricity. From 11:00 to 16:00 the community is a net producer of electricity, and this electricity is accommodated in the battery; in all battery operations the battery is at $SOC_{\min}$ at the start of the surplus PV period. Since the available battery capacity is larger than the surplus PV on this day, the battery can be additionally charged during the surplus PV period, namely between 13:00 and 14:00, when costs and emissions are relatively low.

Fig. 6 shows the impact of the round-trip efficiency on the pareto frontier. It becomes apparent that efficiency is a key factor for the potential on saving costs and emissions. This finding advocates using a battery technology with a high efficiency, for example a Lithium Titanate (LTO) [39], but evidently more factors need to be considered. When efficiency is 77%, the pareto frontier almost intersects the "No Battery" reference case, which would make simultaneously saving costs and emissions impossible.

C. Load Flow Analysis

Figs. 7 and 9 show the transformer loading, line loading and minimum and maximum voltage, respectively, over the 295 days at 5-minute time resolution, for the balanced operation scenario; the other scenarios render similar results. The results show that LV grid limits were not violated in the load flow simulations. The maximum transformer loading was 140 kVA, or 87.3% of its capacity. This occurs when there is surplus PV electricity generation and simultaneously the battery is exporting electricity to the grid. However, because the grid limits in the optimization

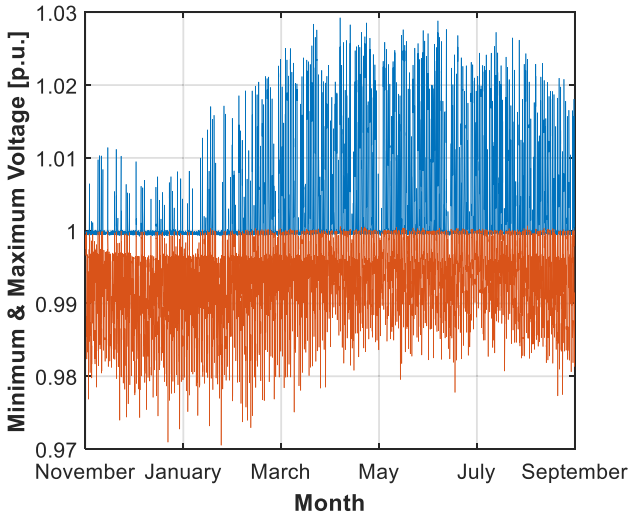

Fig. 9. Minimum and maximum voltage at all nodes at 5-minutes time resolution for the balanced schedule.

model were set at 83.7 kWh/h (see Section II.C.5), no transformer loading problems occur. Similarly, the line loading stays well within the limits with a maximum loading of 58.4%. Lastly, the voltage analysis of all nodes in the network shows voltages stay well within the limits as defined by EN-50160, which are $+0.10$ p.u. and -0.15 p.u. for 10-minute average values over a year [40]. Maximum voltage over 5 minutes found was 1.03 p.u. and minimum 0.97 p.u.

IV. Conclusion

In this paper a framework is proposed that enables the multi-objective optimization of cost and emissions by making use of a CES system. Our method ensures that the self-consumption levels of PV-generated electricity are not hampered. The analysis shows that costs and emissions can simultaneously be decreased compared to reference cases without a CES and with a CES only focused on self-consumption. We have found very attractive, even negative, CO_2 abatement costs. Various schedules show low CO_2 pay-back times of fewer than three years. Our framework enables households that co-own a CES to decide between the trade-off of costs and emissions. We also show that the (dis)charging schedules do not exceed LV grid limitations.

Some considerations are required when implementing the proposed framework in practice. First, forecast errors could result in different economic results than presented here. The load forecast errors present a practical problem for all traders; the trade-off between profit maximization and risk acceptance. Further elaboration for future work could include hierarchical optimization, i.e., after the DAM optimization, proceed to closer to real-time markets (i.e., supporting multi-revenue streams), or first intra-day markets and then in balancing markets where the hierarchical control compensates for forecast errors by exploiting the real-time balancing market (see e.g., [15]). PV electricity generation forecast errors on the other hand, could results in too much or too few capacity of the CES being reserved for accommodating PV-generated electricity. State-of-the-art machine learning methods have an average day-ahead mean absolute error of six to seven percent for forecasts of hourly totals [41]; operators of a CES could decide to reserve some capacity of the battery to ensure high self-consumption rates. However, forecast errors only slightly affect the Pareto curve, as we found in preliminary work, and the overall results still hold clearly. This is also confirmed in recently published work [42].

The focus of our paper is on operational aspects and excludes construction, finance and end-of-life. Future research could include these, to determine under what economic circumstances investing in a CES becomes a business case. Furthermore, not all factors influencing battery degradation are taken into account. To limit computational time, we considered temperature to be controlled within acceptable range by the battery management system and maximized the C-rate at 0.4 [h^{-1}]. However, these factors could also be included in the battery model for a more accurate analysis of battery degradation. A further option is to increase the level of detail in the load flow analysis, e.g., increase the time resolution, and to make it part of optimization model.

The proposed framework can be extended in several directions. First, the trade-offs between emissions and other price incentives can be investigated. Examples are operation on the reserve markets such as Frequency Containment Reserve or Frequency Restoration Reserve. In addition, our framework can be applied to a variety of cases of optimizing flexible resources, such as electric vehicles, heat pumps and industrial electricity loads.

To conclude, in a medium- to long-term future CES systems could even be price setters in electricity spot markets. This could inspire new research, for example on exploring possible bidding strategies of aggregators operating CES systems, but also on how to quantify the marginal emissions of storage systems.

Acknowledgment

The Authors would like to thank David Reihs and Stefan Übermasser from the Austrian Institute of Technology for the discussions leading up to this work. The authors would also like to thank DNV GL, AmersVolt and Icasus for data provision.

References

[1] T. AlSkaif, A. C. Luna, M. G. Zapata, J. M. Guerrero, and B. Bellalta, "Reputation-based joint scheduling of households appliances and storage in a microgrid with a shared battery," *Energy Build.*, vol. 138, pp. 228–239, 2017.

[2] G. Masson, J. I. Briano, and M. J. Baez, "Review and analysis of PV self-consumption policies," IEA PVPS, Paris, 2016.

[3] O. Schmidt, A. Hawkes, A. Gambhir, and I. Staffell, "The future cost of electrical energy storage based on experience rates," *Nature Energy*, vol. 6, 2017, Art. no. 17110.

[4] S. van der Stelt, T. AlSkaif, and W. van Sark, "Techno-economic analysis of household and community energy storage for residential prosumers with smart appliances," *Appl. Energy*, vol. 209, pp. 266–276, 2018.

[5] D. Parra *et al.*, "An interdisciplinary review of energy storage for communities: Challenges and perspectives," *Renew. Sustain. Energy Rev.*, vol. 79, pp. 730–749, 2017.

[6] I. Naziri Moghaddam, B. H. Chowdhury, and M. Doostan, "Optimal sizing and operation of battery energy storage systems connected to wind farms participating in electricity markets," *IEEE Trans. Sustain. Energy*, vol. 10, no. 3, pp. 1184–1193, Jul. 2019.

[7] D. Parra, S. A. Norman, G. S. Walker, and M. Gillott, "Optimum community energy storage system for demand load shifting," *Appl. Energy*, vol. 174, pp. 130–143, 2016.

[8] P. R. Thomas, T. J. Walker, and C. A. McCarthy, "Demonstration of community energy storage fleet for load leveling, reactive power compensation, and reliability improvement," in *Proc. IEEE Power Energy Soc. General Meeting*, 2012, pp. 1–4.

[9] A. Taşcikaraoğlu, N. G. Paterakis, O. Erdinç, and J. P. S. Catalão, "Combining the flexibility from shared energy storage systems and DLC-based demand response of HVAC units for distribution system operation enhancement," *IEEE Trans. Sustain. Energy*, vol. 10, no. 1, pp. 137–148, Jan. 2019.

[10] M. Nasir, H. A. Khan, A. Hussain, L. Mateen, and N. A. Zaffar, "Solar PV-based scalable DC microgrid for rural electrification in developing Regions," *IEEE Trans. Sustain. Energy*, vol. 9, no. 1, pp. 390–399, Jan. 2018.

[11] C. Truong, M. Naumann, R. Karl, M. Müller, A. Jossen, and H. Hesse, "Economics of residential photovoltaic battery systems in Germany: The case of Tesla's powerwall," *Batteries*, vol. 2, no. 2, pp. 1–17, 2016.

[12] J. Hoppmann, J. Volland, T. S. Schmidt, and V. H. Hoffmann, "The economic viability of battery storage for residential solar photovoltaic systems—-A review and a simulation model," *Renew. Sustain. Energy Rev.*, vol. 39, pp. 1101–1118, 2014.

[13] W. L. Schram, I. Lampropoulos, and W. G. J. H. M. Van Sark, "Photovoltaic systems coupled with batteries that are optimally sized for household self-consumption: Assessment of peak shaving potential," *Appl. Energy*, vol. 223, pp. 69–81, 2018.

[14] M. Stadler *et al.*, "Value streams in microgrids: A literature review," *Appl. Energy*, vol. 162, pp. 980–989, 2016.

[15] I. Lampropoulos, W. L. Kling, P. Garoufalis, and P. P. J. van den Bosch, "Hierarchical predictive control scheme for distributed energy storage integrated with residential demand and photovoltaic generation," *IET Gener. Transm. Distrib.*, vol. 9, no. 15, pp. 2319–2327, 2015.

[16] G. B. M. A. Litjens, E. Worrell, and W. G. J. H. M. van Sark, "Economic benefits of combining self-consumption enhancement with frequency restoration reserves provision by photovoltaic-battery systems," *Appl. Energy*, vol. 223, pp. 172–187, 2018.

[17] B. S. Palmintier and M. D. Webster, "Impact of operational flexibility on electricity generation planning with renewable and carbon targets," *IEEE Trans. Sustain. Energy*, vol. 7, no. 2, pp. 672–684, Apr. 2016.

[18] P. Vithayasrichareon, G. Mills, and I. F. Macgill, "Impact of electric vehicles and solar pv on future generation portfolio investment," *IEEE Trans. Sustain. Energy*, vol. 6, no. 3, pp. 899–908, Jul. 2015.

[19] R. L. Fares and M. E. Webber, "The impacts of storing solar energy in the home to reduce reliance on the utility," *Nature Energy*, vol. 2, 2017, Art. no. 17001.

[20] C. X. Wu, C. Y. Chung, F. S. Wen, and D. Y. Du, "Reliability/cost evaluation with PEV and wind generation system," *IEEE Trans. Sustain. Energy*, vol. 5, no. 1, pp. 273–281, Jan. 2014.

[21] K. Deb, *Multi-Objective Optimization Using Evolutionary Algorithms*. vol. 16. Hoboken, NJ, USA: Wiley, 2001.

[22] M. D. Somma, G. Graditi, E. Heydarian-Forushani, M. S.-khah, and P. Siano, "Stochastic optimal scheduling of distributed energy resources with renewables considering economic and environmental aspects," *Renew. Energy*, vol. 116, pp. 272–287, 2018.

[23] A. Fleischhacker, G. Lettner, D. Schwabeneder, and H. Auer, "Portfolio optimization of energy communities to meet reductions in costs and emissions," *Energy*, vol. 173, pp. 1092–1105, 2019.

[24] B. Lokeshgupta and S. Sivasubramani, "Multi-objective dynamic economic and emission dispatch with demand side management," *Int. J. Elect. Power Energy Syst.*, vol. 97, pp. 334–343, 2018.

[25] J. Wang *et al.*, "Degradation of lithium ion batteries employing graphite negatives and nickelecobaltemanganese oxide þ spinel manganese oxide positives: 1, aging mechanisms and life estimation," *J. Power Sources*, vol. 272, pp. 1154–1161, 2014.

[26] D. I. Stroe, M. Swierczynski, A. I. Stan, R. Teodorescu, and S. J. Andreasen, "Accelerated lifetime testing methodology for lifetime estimation of lithium-ion batteries used in augmented wind power plants," *IEEE Trans. Ind. Appl.*, vol. 50, no. 6, pp. 4006–4017, Nov./Dec. 2014.

[27] M. A. Miner, "Cumulative damage in fatigue," *J. Appl. Mech.*, vol. 12, no. 3, pp. A159–A164, 1945.

[28] I. Laresgoiti, S. Käbitz, M. Ecker, and D. U. Sauer, "Modeling mechanical degradation in lithium ion batteries during cycling: Solid electrolyte interphase fracture," *J. Power Sources*, vol. 300, pp. 112–122, 2015.

[29] M. Ecker *et al.*, "Calendar and cycle life study of Li(NiMnCo)O2-based 18650 lithium-ion batteries," *J. Power Sources*, vol. 248, pp. 839–851, 2014.

[30] J. Hooker, G. Ottosson, E. S. Thorsteinsson, and H. J. Kim, "Scheme for unifying optimization and constraint satisfaction methods," *Knowl. Eng. Rev.*, vol. 15, no. 1, pp. 11–30, 2000.

[31] G. Kerber, *Aufnahmefähigkeit von Niederspannungsverteilnetzen für die Einspeisung aus Photovoltaikkleinanlagen*. München, Germany: Technische Universität München, 2011.

[32] P. van Oirsouw, *Netten Voor Distributie Van Elektriciteit*. Arnhem, The Netherlands: Phase to Phase, 2011.

[33] "Smart Grid: rendement voor iedereen," 2017. [Online]. Available: http://www.smartgridrendement.nl/. Accessed on: Aug. 21, 2017.

[34] EPEX SPOT, "EPEX SPOT—Welcome," 2018. [Online]. Available: https://www.apxgroup.com/

[35] R. Harmsen and W. Graus, "How much CO_2 emissions do we reduce by saving electricity? A focus on methods," *Energy Policy*, vol. 60, pp. 803–812, 2013.

[36] W. Schram, I. Lampropoulos, T. Alskaif, and W. Van Sark, "On the use of average versus marginal emission factors," in *Proc. 8th Int. Conf. Smart Cities Green ICT Syst. (SMARTGREENS 2019)*, 2019, pp. 187–193.

[37] L. A. W. Ellingsen, G. Majeau-Bettez, B. Singh, A. K. Srivastava, L. O. Valøen, and A. H. Strømman, "Life cycle Assessment of a Lithium-Ion battery vehicle pack," *J. Ind. Ecol.*, vol. 18, no. 1, pp. 113–124, 2014.

[38] C. Campestrini, P. Keil, S. F. Schuster, and A. Jossen, "Ageing of lithium-ion battery modules with dissipative balancing compared with single-cell ageing," *J. Energy Storage*, vol. 6, pp. 142–152, 2016.

[39] IRENA, *Electricity Storage and Renewables: Costs and Markets to 2030*, Int. Renewable Energy Agency, Abu Dhabi, 2017.

[40] NEN-EN, *50160 - Voltage Characteristics of Electricity Supplied by Public Electricity Networks*. Nederlands Normalisatie-instituut – Europese normen (Dutch Standardization Institute – European Norms), The Netherlands, 2010.

[41] L. Visser, T. Alskaif, and W. Van Sark, "Benchmark analysis of day-ahead solar power forecasting techniques using weather predictions," in *Proc. IEEE Photovolt. Specialist Conf.*, 2019.

[42] I. Lampropoulos, T. Alskaif, J. Blom, and W. van Sark, "A framework for the provision of flexibility services at the transmission and distribution levels through aggregator companies," *Sustain. Energy, Grids Networks*, vol. 17, 2019.

[43] J. Weniger, T. Tjaden, and V. Quaschning, "Sizing of residential PV battery systems," *Energy Procedia*, vol. 46, pp. 78–87, 2014.

[44] Tesla, "Tesla powerwall 2 AC aatasheet," 2018. [Online]. Available: https://www.tesla.com/sites/default/files/pdfs/powerwall/Powerwall2_AC_Datasheet_en_northamerica.pdf. Accessed on: Apr. 19, 2018.

[45] T. S. Schmidt *et al.*, "Additional emissions and cost from storing electricity in stationary battery systems," *Environ. Sci. Technol.*, vol. 53, pp. 3379–3390, 2019.